JOURNAL OF GEOPHYSICAL RESEARCH, VOL. 106, NO. A12, PAGES 29,555–29,569, DECEMBER 1, 2001

Cusp ion steps, field-aligned currents and poleward moving auroral forms

M. Lockwood,[1,2] S. E. Milan,[3] T. Onsager,[4] C.H.Perry,[2] J.A. Scudder,[5]
C. T. Russell,[6] and M. Brittnacher[7]

Abstract. We predict the field-aligned currents around cusp ion steps produced by pulsed reconnection between the geomagnetic field and an interplanetary magnetic field (IMF) with a B_Y component that is large in magnitude. For $B_Y > 0$, patches of newly opened flux move westward and eastward in the Northern and Southern Hemispheres, respectively, under the influence of the magnetic curvature force. These flow directions are reversed for $B_Y < 0$. The speed of this longitudinal motion initially grows with elapsed time since reconnection, but then decays as the newly opened field lines straighten. We predict sheets of field-aligned current on the boundaries between the patches produced by successive reconnection pulses, associated with the difference in the speeds of their longitudinal motion. For low elapsed times since reconnection, near the equatorward edge of the cusp region where the field lines are accelerating, the field-aligned current sheets will be downward or upward in both hemispheres for positive or negative IMF B_Y, respectively. At larger elapsed times since reconnection, as events slow and evolve from the cusp into the mantle region, these field-aligned current directions will be reversed. Observations by the Polar spacecraft on August 26,1998, show the predicted upward current sheets at steps seen in the mantle region for IMF $B_Y > 0$. Mapped into the ionosphere, the steps coincide with poleward moving events seen by the CUTLASS HF radar. The mapped location of the largest step also coincides with a poleward moving arc seen by the UVI imager on Polar. We show that the arc is consistent with a region of upward field-aligned current that has become unstable, such that a potential drop of about 1 kV formed below the spacecraft. The importance of these observations is that they confirm that the poleward moving events, as seen by the HF radar and the UV imager, are due to pulsed magnetopause reconnection. *Milan et al.* [2000] noted that the great longitudinal extent of these events means that the required reconnection pulses would have contributed almost all the voltage placed across the magnetosphere at this time. The observations also show that auroral arcs can form on open field lines in response to the pulsed application of voltage at the magnetopause.

1. Introduction

Recent studies by *Milan et al.* [2000] (hereinafter referred to as MEA) have revealed signatures in global UV auroral images that are coincident with poleward moving events detected using HF coherent radar. These signatures are consistent with the predicted effects of pulsed magnetic reconnection in the magnetopause current layer when the interplanetary magnetic field (IMF) has a southward component. The most significant feature of the events presented by MEA is their large longitudinal extent, which the satellite-based imager shows to be at least 5 hours of magnetic local time (MLT). This means that if the interpretation in terms of pulsed reconnection is correct, individual events can contain a significant fraction (of the order of 10%) of the total open magnetic flux in the polar cap and that they contribute almost all the voltage placed across the magnetosphere. In this paper we present observations of the ion precipitation that confirm that the events are indeed due to pulses in the reconnection rate: These data also help explain the formation of these UV arcs on the newly opened field lines. Thus we confirm the conclusion of MEA that reconnection pulses contribute almost all of the transpolar voltage at this time, as argued for previous events by *Lockwood et al.* [1990, 1993a, 1993b] and *Lockwood* [1994] but which was considered to be impossible by *Newell and Sibeck* [1993]. (See also discussion by *Lockwood et al.* [1995b].) In this introduction we briefly review the signatures at the magnetopause and in the ionosphere that are thought to be caused by pulsed magnetopause reconnection. We place particular emphasis on the extent of events in local time.

1.1. Magnetopause Signatures of Pulsed Reconnection

Pulsed magnetic reconnection in the magnetopause current layer was first invoked by *Russell and Elphic* [1978, 1979] and *Haerendel et al.* [1978] to explain a characteristic set of

1 Department of Physics and Astronomy, Southampton University, Southampton, England.
2 Space Science Department, Rutherford Appleton Laboratory, Oxfordshire, England.
3 Department of Physics and Astronomy, Leicester University, Leicester, England.
4 NOAA Space Environment Center, Boulder, Colorado.
5 University of Iowa, Iowa City, Iowa.
6 University of California Los Angeles, Los Angeles, California.
7 Geophysics Program, University of Washington, Seattle, Washington.

Paper number 2000JA900175.
0148-0227/01/2000JA900175$09.00

signatures called "flux transfer events" (FTEs), seen by spacecraft near the magnetopause. This concept subsequently proved very powerful in explaining the statistical occurrence, motion and characteristics of FTEs. However, there are several distinct models that use the concept of pulsed reconnection to explain the FTE signature. The original model, by *Russell and Elphic* [1978], is inherently three-dimensional and invoked a reconnection pulse lasting a short (meaning typically 1 min) interval over a short (meaning typically 1 Earth radius, 1 R_E) reconnection X-line. This generates a tube of newly opened flux that penetrates the magnetopause obliquely, such that an FTE signature is seen over a larger extent of the magnetopause than the short X-line that produced it. Statistical surveys show that FTEs are observed at all local times in the dayside magnetopause with a repeat time that is everywhere close to the average of 8 min [*Lockwood et al.*, 1995b; *Kawano and Russell*, 1996, 1997]. Thus unless one invokes an extreme and unlikely topology, whereby each single tube of newly opened flux is draped over the entire dayside magnetopause, several of these short X-lines (each giving pulsed reconnection) would be required to explain the occurrence of the FTE signatures at all local times. (In other words, the reconnection would need to be patchy as well as sporadic.)

In contrast, the model of FTE signatures proposed by *Southwood et al* [1988] and modeled by *Scholer* [1988, 1989] is inherently two-dimensional. This means that there is cylindrical symmetry along the reconnection X-line, which can be of any length. For this interpretation, there is no information on the length of the X-line in the signature seen by a satellite. This is because the satellite samples field lines opened at just one segment of the X-line. *Lockwood et al.* [1995b] studied the occurrence frequency and size of FTEs as a function of MLT and concluded that for this two-dimensional model, FTEs contributed almost all of the antisunward transport of open flux. This being the case, FTEs would not only be the dominant contribution to magnetosphere-ionosphere convection, but also they would be sufficient to explain even the largest of observed transpolar voltages. This conclusion would be true independent of the length of the X-line (or X-lines) producing the events and thus of the size of the individual patches of newly opened flux that they produced. However, if the X-lines are short, there must be many of them.

Lockwood and Hapgood [1998] have reviewed all the viable models of FTEs and carried out a detailed analysis of one event that has been interpreted in terms of each theory. They used the ion data to show that the event contains newly opened field lines that were indeed produced by a pulse in the reconnection rate. They show that the observed evolution of the ions on the event boundaries were consistent only with the two-dimensional pulsed reconnection model. This implies that the conclusions of *Lockwood et al.* [1995b] apply and that FTEs are the dominant contribution to convection.

Lockwood et al. [1995b] noted that the reconnection X-line need not be static in this two-dimensional pulsed reconnection model. This concept was suggested by *Lockwood et al.* [1993b] and *Lockwood* [1994] in order to explain some of the characteristics of flow bursts in the cusp/cleft ionosphere, thought to be signatures of FTEs (see the next section). A short, active X-line segment could propagate over the magnetopause, generating newly opened flux as it goes. The X-line could then be active for considerable total intervals (of the order of 10-15 min), but the reconnection at every location over which it passes would last only the short interval (about 1 min) needed to explain the FTE signatures. The resulting patch of newly opened flux is much more extensive in MLT than the X-line was at any one time. The reconnection is pulsed at any one location, but given that one traveling enhancement could form before the prior one had died out, reconnection could still be continuously present in the magnetopause. The ionospheric observations of MEA support this concept.

1.2. Ionospheric Signatures of Pulsed Reconnection

Poleward moving transient events, seen at wavelengths of 630 and 557.7 nm, have been shown by ground-based measurements to be the normal behavior of the cusp/cleft aurora when the IMF has a southward component [e.g., *Sandholt et al.*, 1992; *Fasel*, 1995]. Observations by the European Incoherent Scatter (EISCAT) UHF and VHF radars showed that these auroral transients were colocated in space and time with transient flow bursts, revealing transient momentum transfer across the magnetopause [*Lockwood et al.*, 1989a, 1989b, 1993a, 1993b; *Moen et al.*, 1995, 1996] and the consequent heating of the ionospheric ion gas [*Lockwood et al.*, 1993a, 1995a]. The longitudinal motion of the transient auroral events also supports the idea that they are patches of newly opened flux, moving westward (in the Northern Hemisphere) when the IMF B_Y component is positive and eastward when it is negative [*Sandholt et al.*, 1992; *Lockwood et al.*, 1993a]: The only known explanation of this pattern of motion is the curvature ("tension") force on the newly opened field lines, and the repetitive pattern of formation and motion of these events shows that patches of such field lines are produced by pulses in the reconnection rate [*Lockwood et al.*, 1995a]. This pattern of event motion is also consistent with the asymmetric MLT distributions of their occurrence for $B_Y > 0$ and $B_Y < 0$ [*Karlson et al.*, 1996].

Lockwood et al. [1990] used the duration and speeds of the flow bursts at a meridian and deduced that at least some of the patches of newly opened flux must be extensive in longitude (over about 2000 km), meaning that they could form flow channels that cover over 4 hours in magnetic local time. These authors also deduced that these event had large longitudinal extent from the small magnitudes of any return flows outside the events. *Pinnock et al.* [1993] imaged the transient flow channels with the Halley Bay HF coherent scatter radar and showed they could indeed extend over the whole of their field of view (i.e., more than about 1000 km). *Rodger et al.* [1995] and *Milan et al.* [1999] have shown that these poleward moving flow channels are associated with poleward moving 630-nm optical transients. However, the flow channels are more easily seen by the HF radars away from the winter solstice conditions that are required to detect the auroral transients and hence combined observations remain relatively rare. Recently, MEA have shown that the flow channels seen by HF radar are also associated with poleward moving forms seen in global images of the UV aurora and that these were up to 2500 km long. The east-west direction of flow in the channels is controlled by the IMF B_Y [*Provan et al.*, 1998] and their motion, as for the optical transients, is consistent with their occurrence as a function of local time [*Provan and Yeoman*, 1999; *Provan et al.*, 1999]. These statistical studies of the flow channels also point to large longitudinal extents.

The large extent of the regions of newly opened flux had been considered controversial. *Newell and Sibeck* [1993] argued that pulsed reconnection could only take place in a localized region, although the traveling transient reconnection pulse scenario proposed by *Lockwood et al.* [1993b, 1995b] is not subject to this limitation [*Lockwood*, 1994]. *Lockwood et al.* [1993a] deduced that 630-nm transients had extents comparable with those discussed above. *Moen et al.* [1995] used all-sky cameras, magnetometers and radars to show that these events modulated the flow in both the dawn and the dusk cell of the convection pattern, implying large longitudinal extent. This modulation was consistent with the idea that ionospheric flow driven by one reconnection pulse persists for an interval of 10-15 min and that the pulses in the reconnection voltage are inductively smoothed in the ionosphere [*Cowley and Lockwood*, 1992; *Cowley et al.*, 1991; *Lockwood*, 1994]. The modulation of the field-aligned currents required to transfer the motion into the ionosphere has been deduced from magnetometer and optical observations by *Øieroset et al.* [1996, 1997].

Other predicted signatures of pulsed reconnection are discontinuities in the dispersion of injected solar wind ions in the cusp region, called "cusp ion steps" [*Cowley et al.*, 1991; *Lockwood and Smith*, 1992; *Escoubet et al.*, 1992; *Lockwood and Davis*, 1996]. Modeling of the effects of pulsed magnetopause reconnection has been shown to reproduce the observed simultaneous steps in both downgoing and upgoing ions in the cusp at middle altitudes, demonstrating that these events are caused by pulsed reconnection and not by pulsed plasma transfer across the magnetopause [*Lockwood et al.*, 1998]. Cusp ion steps at low altitudes have been reported by *Lockwood et al.* [1993c] in association with poleward moving patches of elevated electron temperature, detected by incoherent scatter radar. They have also been seen with poleward moving cusp/cleft auroral transients by *Farrugia et al.* [1998]. *Pinnock et al.* [1995] found the poleward moving flow channels (detected by HF radar) were in association with a seemingly different "sawtooth" signature in the cusp ions at low altitudes. However, *Lockwood and Davis* [1996] showed that this sawtooth signature was, in fact, the same phenomenon as the cusp ion steps seen by *Lockwood et al.* [1993c] – the differences arising purely from the longitudinal nature of the satellite pass studied by Pinnock et al., as opposed to the more meridional pass studied by Lockwood et al. At middle and high altitudes, the theory predicts that pulsed reconnection will produce only the sawtooth signatures (*Lockwood et al.*, 1998). Note that the same theory was also used by *Lockwood and Hapgood* (1998) to successfully model the ions observed during a magnetopause FTE signature.

1.3. Joint Ionospheric and Magnetopause Observations of FTEs

Opportunities to make simultaneous measurements of these ionospheric and magnetopause signatures have been extremely rare. The evidence that both sets of signatures are indeed produced by pulsed reconnection is, in our view, overwhelming. However, we do not yet know if the reconnection pulses that generate the ionospheric signatures are the same (in terms of amplitude, duration, reconnection site and longitudinal extent) as those that generate the magnetopause FTE signatures.

Only two such sets of combined observations have been made to date. On both occasions an association was found. This is despite the difficulties and ambiguities in interpreting the data from the experiment, which was complicated by magnetopause motions. This is because the occurrence of FTE signatures is modulated by the distance between the satellite and the current layer, which varies rapidly as the boundary moves in and out. The first set of combined observations was made shortly before the end of ISEE operations, and FTEs at the magnetopause were seen in conjunction with flow bursts seen by the EISCAT radar and auroral transients [*Elphic et al.*, 1990]. Recently, *Neudegg et al.* [1999] have shown magnetopause FTEs seen during the brief operations of the Equator-S satellite were associated with poleward moving flow-channels seen by the Co-operative UK Twin Located Auroral Sounding System (CUTLASS) HF backscatter radar.

1.4. The Relationship of the Various Ionospheric Signatures

Section 1.2 briefly reviews the evidence that pulsed magnetopause reconnection produces poleward moving flow bursts/channels, poleward moving optical transients and cusp ion steps. These have indeed all been detected in association with each other by *Yeoman et al.* [1997]. However, interesting questions remain about the origin of the gaps that separate the poleward moving events [*Davis and Lockwood*, 1996; *Lockwood et al.*, 2000] and how one signature relates to another.

The 557.7nm-dominant part of the auroral transients studied by *Lockwood et al.* [1993a] was coincident with an inferred sheet of upward field-aligned current: This was one of the oppositely directed pair on the edges of the flow channel. This pair of field-aligned currents is required to transfer the motion of the newly opened flux into the ionosphere [*Southwood*, 1985, 1987]. The poleward moving UV aurorae observed by MEA also appear to be associated with this region of upward field-aligned current. The cusp ion steps show that patches of newly opened flux are appended to each other in a contiguous manner [*Cowley at al.*, 1991; *Lockwood and Smith*, 1992]. The electron precipitation, on the other hand, appears to be more structured, the more mobile electrons being responsible for most of the required field-aligned currents and for maintaining the quasi-neutrality of the plasma [*Burch*, 1985]. In the next section we consider theoretically the field-aligned currents associated with a series of these contiguous patches of newly opened flux for when the IMF B_Y component is large in magnitude.

2. Field-Aligned Currents at Cusp Ion Steps

Consider a coordinate system with the Z axis aligned with the magnetic field $\boldsymbol{B}$, and the Y axis aligned with a long cusp ion step. Cusp ion steps are "adiaroic" boundaries (meaning "not flowing across," i.e., they move with the convection velocity of the surrounding plasma) [*Siscoe and Huang*, 1985]. Thus the boundary-normal velocity v_X and the tangential electric field E_Y are zero in the boundary rest frame. If the boundary is idealized to be infinitely long, the field-aligned current in the boundary, $J_\parallel$, does not vary with y and so causes a tangential magnetic perturbation $dB = dB_Y$. From Ampere's law, applied to a slab in the ionosphere of field-perpendicular area ($dXdY$), we find ($J_\parallel dX$) is equal to ($2dB_Y/\mu_o$). Applying current continuity to the same volume, we find ($J_\parallel dX$) is also equal to dI_X, where I is the height-integrated field-perpendicular ionospheric current. Thus

$$J_{\parallel} = (2/\mu_o)dB_Y/dX = dI_X/dX = d(\Sigma_P E_X)/dX = (-1/B)d(\Sigma_P v_Y)/dX = -(\Sigma_P/B)dv_Y/dX, \quad (1)$$

where we have assumed for simplicity that the Pederson conductivity Σ_P is uniform is space (generalization is straightforward but cumbersome) and that $B >> dB$. This yields $dB_Y = -(\mu_o\Sigma_P / 2B)dv_Y$, and integrating this with respect to distance along a satellite path to a given point gives $B_Y = -(\mu_o\Sigma_P / 2B)v_Y + c$. If $v_Y = 0$, B_Y is the undisturbed field B_{YO}, and thus $c = B_{YO}$ and

$$\Delta B_Y = B_Y - B_{YO} = -(\mu_o\Sigma_P / 2B)v_Y . \quad (2)$$

Thus the magnetic deflection tangential to the boundary will be proportional to the tangential velocity. Note that this is the deflection due to the field-aligned currents only. This would equal the total magnetic deflection at sufficiently great altitudes to make the contribution of field-perpendicular ionospheric currents negligible.

Consider a satellite moving such that it passes through a cusp ion step at speed V_s in the Earth's frame of reference. The boundary-normal convection velocity V_c will equal the speed of motion of this adiaroic boundary, V_b, also measured in the Earth's frame. If we define V_s, V_b and V_c to be positive in the $+X$ direction, the satellite velocity in the $+X$ direction in the boundary frame of reference is $dX/dt_s = (V_s - V_b)$, thus from (1)

$$dB_Y/dt_s = (\mu_o/2)(V_s - V_b) J_{\parallel} \quad (3)$$

Thus the gradient of the observed field with observation time t_s depends not only on $J_{\parallel}$ but also on $(V_s - V_b)$. In fact, if $V_s < V_c = V_b$ (which means that an adiaroic boundary was observed because it convected over the spacecraft, rather than because the spacecraft moving though it), even the polarity of an inferred field-aligned current is reversed compared with what would be inferred from the observed change in field if the boundary is assumed to be static and the satellite moved through it with $V_s > V_b = 0$. As a result, field-aligned currents deduced from satellite magnetometer data may often have been ascribed incorrect magnitudes, and even polarities, if the effect of their motion was not recognized.

Consider the highly idealized square patch of newly opened magnetic flux in the Northern Hemisphere shown in Figure 1a. This would be produced by a very short pulse of very fast reconnection between closed geomagnetic flux and a magnetosheath field that has a large positive Y component in the GSM frame of reference. Because the pulse was very short, all field lines in the patch were reconnected at almost the same time, t_o, and so elapsed time since reconnection $(t_o - t_s)$ is uniform in the patch at any one observation time t_s. The northward (poleward) direction is toward the bottom of the figure, and the patch moves westward (to the right) with speed V_w under the influence of the curvature force. Figure 1a illustrates the resulting plasma flows, Pedersen currents and field-aligned currents associated with this westward motion [*Southwood*, 1985, 1987]. Figure 1b considers the superposition of the field-aligned currents associated with three such idealized patches, opened in the order 1, 2, 3. Apart from very early in the event's lifetime, the tension force on each set of flux tubes decays with increasing time elapsed since reconnection $(t_o - t_s)$, as the newly opened field lines straighten and evolve into the tail lobe [*Saunders*, 1989]. Thus we consider $V_{w3} > V_{w2} > V_{w1}$ and the field-aligned currents required for event 1 are less than for events 2 and 3. An important facet of

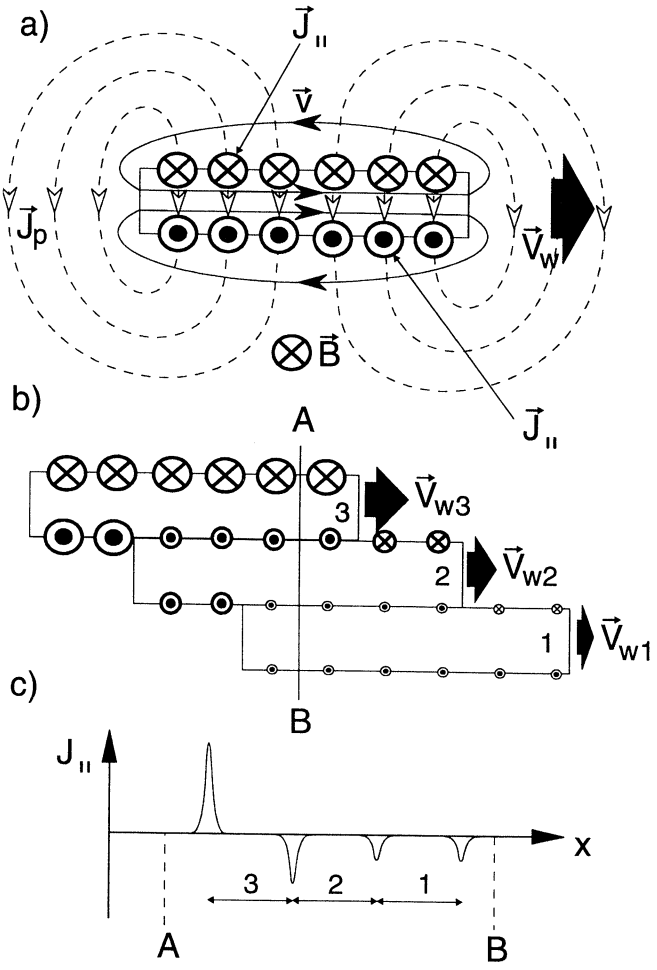

Figure 1. Schematic of field-aligned currents for idealized patches of newly opened flux in the Northern Hemisphere produced by reconnection rate pulses with an interplanetary magnetic field (IMF) that has a large positive B_Y component. For simplicity, the pulse length is taken to approach zero so that all field lines within the patch are opened simultaneously and are moving with the same velocity at any one time. (a) The flows, Pedersen currents and field-aligned currents associated with the westward motion ($\underline{V_W}$) of an isolated patch. (b) Three patches like that in Figure 1a, reconnected in the order 1, 2 and 3 such that $V_{W3} > V_{W2} > V_{W1} > 0$. (c) The variation of field-aligned current (positive being downward) $J_{\parallel}$ along the meridian AB in Figure 1b.

cusp ion steps is that these patches of newly opened flux are appended immediately adjacent to each other, and thus, where they overlap in local time, the upward current on the poleward edge of the newer event would be needed in the same location as the smaller downward current associated with the equatorward edge of the prior event. In such places the sum of the two, a weaker upward current, is seen. This is illustrated schematically in Figure 1b. Note that the conductivities within each patch may also evolve with time elapsed since reconnection and this would be an additional complicating factor. Along the meridian AB in Figure 1b we would have the latitudinal structure in $J_{\parallel}$ that is shown in Figure 1c with a single large downward current being matched by a series of increasingly smaller upward currents. The thin sheets of upward field-aligned current will be coincident with the cusp

ion steps between the patches. The westward motion and the polarity of the field-aligned currents would reverse if the IMF B_Y was negative. For events in the Southern Hemisphere the senses of both the longitudinal flow and of the magnetic field are reversed compared with those in the Northern Hemisphere, and so the directions of the electric fields, Pedersen currents and field-aligned currents, for a given polarity of the IMF B_Y, remain the same.

If we reduce to zero both the duration of the reconnection pulses considered in Figure 1 and the gaps between them, we obtain the steady state limit. This is sketched in Figure 2 for a poleward moving satellite ($V_s > 0$). Figure 2a shows the precipitating ion spectrum, which depends on elapsed time since reconnection (t_o- t_s), as modeled by *Onsager et al.* [1993] and *Lockwood* [1995, 1997]. Because this is a steady state case, the (t_o- t_s) increases linearly with observation time t_s. We allow for the westward velocity V_W increasing initially (with the arrival of the Alfvén wave), but subsequently decaying as (t_o- t_s) increases because the field lines straighten (Figure 2b). This gives the continuous variation of $J_\parallel$ and ΔB sketched in Figures 2c and 2d. From (2), the variation of ΔB and V_W will be the same and, from the above, will depend on (t_o- t_s), as do the ion precipitation characteristics.

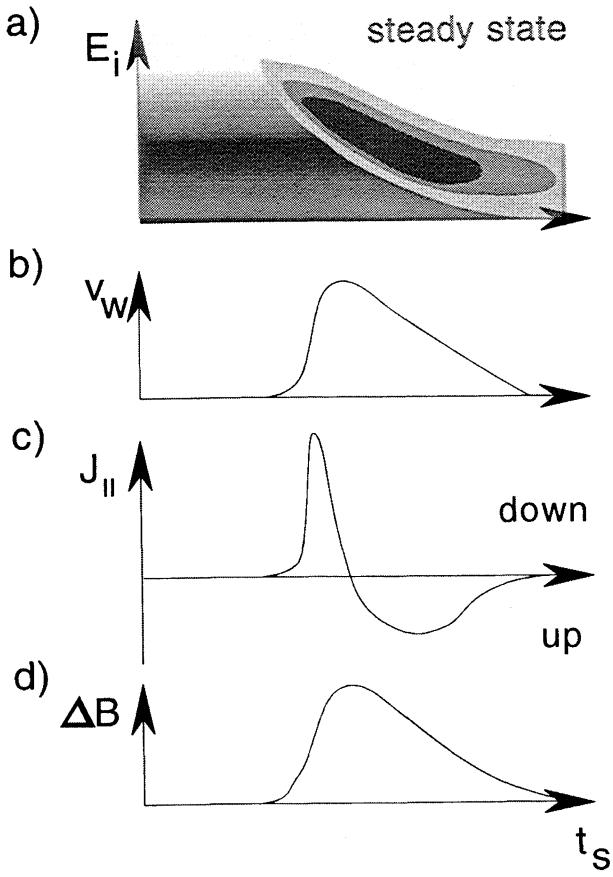

Figure 2. Schematic of predicted variations for a poleward pass ($V_s > 0$) through a steady state cusp. (a) The differential energy flux of field-aligned ions, in an energy-observation time (E_I - t_s) spectrogram format. (b) The westward convection velocity, V_W . (c) The field-aligned current density $J_\parallel$ (positive downward) and the magnetic perturbation ΔB.

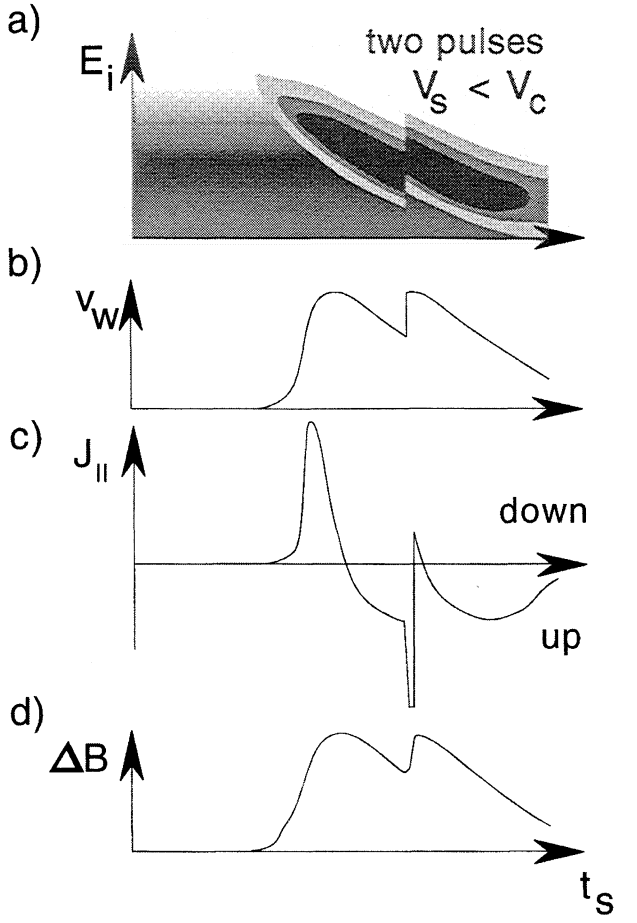

Figure 3. Same as Figure 4 but for a cusp produced by two reconnection pulses with the convection velocity exceeding the satellite velocity ($V_c > V_s > 0$).

Figure 3 generalizes this situation for two reconnection pulses, in the case where $V_c > V_s > 0$. The ion dispersion signature (Figure 3a) shows an upward step corresponding to the interval of zero reconnection, as explained and modeled by *Lockwood et al.* [1998]. Essentially the variation is caused by the variation of elapsed time since reconnection (t_o- t_s) of the field lines that are sampled by the satellite. Because they are also functions of (t_o- t_s), there will be corresponding steps in both ΔB and V_W and an upward current filament at the step, as in Figure 1b. If the current sheet had no width, the value of $J_\parallel$ at the step would go to infinity. We assume in Figure 3c that this sheet of field-aligned current does have a nonzero width and the upward step in ΔB is structured accordingly.

From the above, we predict sheets of field-aligned current on the boundaries between patches (i.e., at the cusp ion steps), associated with the difference in the speeds of their longitudinal motion. For low elapsed times since reconnection, near the equatorward edge of the cusp region where the field lines are accelerating longitudinally, the field-aligned current sheets will be downward/upward in both hemispheres for positive/negative IMF B_Y. At larger elapsed times since reconnection, as events slow and evolve from the cusp into the mantle region, these field-aligned currents will reverse and so be upward/downward in both hemispheres for positive/negative B_Y.

3. Polar Observations of August 26, 1998

With the considerations of section 2 in mind, we study a pass by the Polar satellite on August 26, 1998. This interval has been studied by MEA, who observed extensive, poleward moving auroral arcs at UV wavelengths in the northern polar cap, in association with poleward moving events seen by HF radar. These authors suggest that the UV arcs are the regions of upward field-aligned current on the edge of the patches of newly opened flux. These field-aligned currents are responsible for transferring the motion to the ionosphere. This motion is initially westward and so is consistent with the IMF that is observed to have $B_Z < 0$ and $B_Y > 0$ at the time relevant to the formation of these events. MEA estimate the propagation lag between the Wind spacecraft and the magnetopause is 20-25 min: Here we are mainly concerned with events at 1000-1100 UT, for which the relevant IMF observations were made by Wind at about 0935-1040 UT. Figure 1 of MEA shows that in this interval Wind observed an IMF B_Z component that fluctuated around –10 nT, with B_Y that averaged roughly +10 nT. The UV arc observed by MEA was in the same location, relative to the main patch of red-line emission and the enhanced flow channel, as the green-dominant transient arc in the event studied by *Lockwood et al.* [1993a] and as the low-altitude (~100 km) electron density enhancements observed using the tomographic technique by *Walker et al.* [1998]. We here analyze the insitu data from Polar on this day to search for consistent signatures of cusp ion steps and upward field aligned current, as predicted in Figure 3.

Plate 1 shows the ion observations by the Charge and Mass Magnetospheric Ion Composition Experiment (CAMMICE) instrument at 0600-1300 UT on this day. The observed differential number fluxes J are shown as a function of energy and observation time t_s for various ion species. Initially, the particle data are indicative of the polar cap. At about 0700 UT, the satellite was at a geocentric distance r of 8.7 R_E, an MLT of 0800, and an invariant latitude Λ of 81°. Polar then began to observe spectra characteristic of the magnetosheath (Plate 1e), this origin being confirmed by the fluxes of alpha particles (Plate 1b) and high-charge oxygen ions (of charge 3 and greater; Plate 1a). At 0640UT Wind observed a major increase in the dynamic pressure and a swing of the IMF to northward (see Figure 1 of MEA): These changes appear to have caused the cusp to appear at the Polar satellite at 0700 UT. The predominantly northward orientation of the IMF persisted at Wind until 0925UT. However, at about 0920UT a dispersion ramp commenced in the ion data, showing that Polar was moving onto field lines of larger elapsed time since reconnection (t_o - t_s). This is consistent with the open-closed boundary eroding to lower latitudes, away from the satellite. Prior to 09:20, there is some structure in the sheath precipitation seen by CAMMICE, but this increases considerably after this time. This implies that although the 20 min lag means that the southward turning is not predicted to have reached the magnetopause until about 0945UT, at about 0920UT low-latitude reconnection had begun, and that the structure and the erosion are both associated with this change. Shortly before the southward turning, the B_Y component of the IMF changed from –10 nT to +10 nT, and this could have contributed to a reduction in the propagation delay between Wind and the magnetopause.

After 1010 UT, only weak fluxes were seen above the 1-keV threshold of CAMMICE, showing that the satellite was in the southward-IMF mantle region, although there were brief re-appearances of more significant magnetosheath fluxes near 1040 and 1120 UT. Around 1135 UT, CAMMICE passed rapidly through intense magnetosheath precipitation near r = 5.0 R_E, MLT = 1500, and Λ = 74°. This precipitation has the characteristics of cusp (with high fluxes, high charge state ions, and alpha particles) despite being at such a large MLT, although significant fluxes of energetic magnetospheric ions O^+, O^{2+}, and He^+ (Plates 1c and 1d) were seen here for the first time, and so this intersection could be interpreted as cleft/low-latitude boundary layer (LLBL). Subsequently, Polar passed into the plasma sheet and ring current. The IMF had remained predominantly southward, with only a few brief excursions to northward. In this paper we are interested in the interval when Polar was within the mantle region during southward IMF.

Polar UVI observations of the UV aurora (see section 3.4) were made between 0630 and 1055 UT. Before 0950 (roughly the time when the southward turning of the IMF reached the magnetopause), Polar was at invariant latitudes Λ poleward of 80° (and moved from near 0700 to 1500 in MLT), whereas Plate 1c of MEA shows that at 1500 MLT the main UV aurora was always at $\Lambda < 80°$ (and moving slowly poleward, consistent with the northward IMF). After about 0945, both the UV aurora and the satellite moved equatorward near 1500 MLT, but the satellite footprint did not catch up with the aurora before the end of the UVI observations at 1055 UT. Plate 1 shows that Polar passed through the southward IMF cusp at 1135-1145, after UVI observations had ceased.

3.1. Low-Energy Ions

Plates 2a and 2b show the ions detected by the Hydra instrument on Polar between 1000 and 1115 UT, during this pass. Plate 2a is for ions with pitch angle α_i within 30° of the downward field-aligned direction. The differential energy flux J_E (= JE) of these ions is colour-coded as a function of energy and observation time, t_s. Plate 2b is the same for ions with pitch angle within 30° of the upward field-aligned direction. Downward, precipitating ions are seen up until about 1015 and then again briefly at around 1040. Upward propagating ions are seen throughout the interval. These are mantle ions, originally observed and explained by *Rosenbauer et al.* [1975], mixed with the upgoing ionospheric ions of the cleft ion fountain, as originally observed and explained by *Lockwood et al.* [1985a, 1985b]. The mantle ions have entered along open field lines across the magnetopause, mirrored in the converging magnetic field lines and returned to the satellite while being swept into the tail lobe by antisunward convection. The cleft fountain ions leave the topside cusp ionosphere as thermal flows and are accelerated at altitudes near 1 R_E, close to where the sheath ions are mirrored. They are subsequently also swept antisunward by the convection flow [*Lockwood et al.*, 1985b], such that they obey the same mass, pitch angle and energy dispersions as the mirrored sheath ions. Because the region of upwelling ion acceleration is close to the region where cusp ions mirror in the converging magnetic field lines, cleft ion fountain ions and mirrored mantle ions will obey the same dispersion curve. The ion composition results show there is little flux of O^+ in this region and that the fluxes of He^{++} exceeded those of He^+: This implies that the bulk of the dispersed ion signature is due to injected solar wind and not the ionosphere.

Lockwood [1995, 1997], *Lockwood and Davis* [1996] and *Lockwood et al.* [1998] have discussed how the characteristics of the magnetosheath ion population depend on elapsed time since reconnection, $(t_o - t_s)$. At smaller $(t_o - t_s)$, both downgoing ions and the mirrored upgoing ions can be seen simultaneously. Of the two populations, the upgoing ions will have higher energies, having traveled the larger field-aligned distance from the magnetopause to the mirror point and then back to the satellite than the downgoing ions that have traveled directly from the magnetopause to the satellite. At those times when both upgoing and downgoing populations are detectable, this feature is evident in Plate 2. At larger $(t_o - t_s)$, sheath ions continue to cross the magnetopause along the newly opened field lines but are decelerated on crossing the boundary and then swept into the tail lobe by convection: As a result, very few ions (of very low energy in the Earth's frame) reach the satellite directly from the magnetopause [*Lockwood*, 1995] and the fluxes of the precipitating ions fall below the one-count instrument threshold. However, at such times the satellite can still observe upgoing ions that crossed the magnetopause when $(t_o - t_s)$ was lower and have taken longer to reach the satellite because they have mirrored below it. The cleft fountain ions form a low-energy addition to the mirrored sheath ions. Thus the periods of counterstreaming ions and of only upgoing sheath ions in Plate 2 can both be explained in terms of variations of the time elapsed since reconnection $(t_o - t_s)$ of the field lines that the satellite was observing.

The ions also show sawtooth structures in the dispersion characteristics, with downward ramps separated by upward steps. Cusp ion steps of this form were predicted as a signature of pulsed magnetopause reconnection by *Lockwood and Davis* [1996]. Steps have this sawtooth form if $V_s < V_c$, where V_s and V_c are the components of the satellite and convection velocities, respectively, in the direction of the poleward normal to the open/closed separatrix. *Lockwood et al.* [1998] were able to numerically model simultaneous steps in the up and downgoing ions, proving that these events are due to pulsed reconnection and not pulsed plasma transfer over the magnetopause. In Plate 2b, a sequence of six small upward steps are seen in the interval 1000-1020 UT. Most of these can also be identified in the precipitating ions shown in Plate 2a. Such a rapid repetition, indicating small but frequent reconnection pulses, was also reported by *Lockwood et al.* [1998]. At each upward step, field lines that were reconnected at a later time (i.e., of lower $t_o - t_s$) are convected over the satellite and the satellite begins to observe field lines that were reconnected during a later pulse. Between 1020 and 1035, there may be further steps; however, the ion energy becomes a weak function of $(t_o - t_s)$ at large values and they become difficult to observe. At 1034-1040 a major upward step is seen (labeled A and 1 in Plate 2). This step is structured, and this is discussed in the next three sections. At 1052 and 1101, two more clear upward steps are seen (labeled 2 and 3), followed by an upward ramp (labeled 4) and a small step at 1113 (labeled 5). The upward ramp (4) is well explained by the same theory, the reconnection rate falling to a smaller, but nonzero, value between the pulses. The abruptness of steps 1, 2, 3 and 5 indicates that the reconnection rate fell to undetectably small values. Note that before 1010, $(t_o - t_s)$ is small enough to allow simultaneous steps in both upgoing and downgoing ions, as modeled by *Lockwood et al.*, [1998]. Both the energy and the flux of the magnetosheath ions fall with increasing $(t_o - t_s)$, and they fall faster for larger field-aligned distance from the reconnection site: Thus both are lower for mirrored upgoing ions than for precipitating ions. After 1010 UT, $(t_o - t_s)$ is larger, such that upgoing ions are still seen but precipitating ions have fallen to undetectably low fluxes. The only exception to this statement is at 1040-1043, when step 1 briefly brings field lines of sufficiently low $(t_o - t_s)$ for precipitating ions to be seen, as well as the upgoing ions.

At 1135-1145, when CAMMICE passed through a region of magnetosheath precipitation, the Hydra instrument observed a sequence of four more sawtooth ramps (not shown), showing this region is on newly opened field lines produced by four short pulses of reconnection roughly 2.5 min apart. Thus the presence of some magnetospheric and ionospheric ions (He^+, O^+ and O^{++}; see Plate 1) in this region is not consistent with a closed field line cleft/LLBL interpretation but is consistent with this flank LLBL being on open field lines.

3.2. Electron Observations

Plate 2c and 2d show the differential number fluxes ($J = J_E/E$) of downgoing and upgoing electrons, respectively, with pitch angles α_e within 30° of the field line. Electron fluxes are higher where the ion data reveal lower $(t_o - t_s)$. This is to be expected because quasi-neutrality is maintained [*Burch*, 1985] and the ion (and hence the electron) fluxes decrease with increasing $(t_o - t_s)$ at these large $(t_o - t_s)$. In general, the upgoing and downgoing electron fluxes are similar, much more similar than for the ions, because the difference between upgoing and downgoing times of flight are smaller (the travel time to go from the satellite altitude to the mirror point and back up to the satellite is much smaller for electrons than ions). The major exception to this takes place at 1035-1037 (marked A in Plate 2), close to the large upward step. In this interval, fluxes of downward precipitating electrons remain, but there is a dropout in the fluxes returning upward.

3.3. Magnetic Field Observations

Figure 4 shows the three components of the disturbance magnetic field in the GSM frame of reference, ΔB_X, ΔB_Y, ΔB_Z. In each case the component from the Tsyganenko model has been subtracted from the observed component to show the small-scale variations. The fluctuations in the total disturbance vector ΔB are almost completely normal to the model field direction, consistent with the effects of field-aligned currents. Very small scale structure is seen around the small cusp ion steps earlier in the period, but we here concentrate on that around the largest steps at 1035-1040, 1052 and 1101 UT. In each of these cases the major feature that we see is a bipolar signature in ΔB_Y, with lower ΔB_Y before the step and higher after, as predicted in section 2 for extensive field-aligned current sheets that are aligned close to parallel to the Y axis and moving antisunward over the satellite. The ΔB_Y variations around the steps are similar in form to those predicted in Figure 3 and are found at each of the ion steps in the mantle region identified in Plate 2.

3.4. UV Images

The UVI instrument made observations between 0630 and 1051 UT on this day. The satellite's path keeps it poleward of invariant latitude, Λ, of 83° at 0630-1030 (but moving from

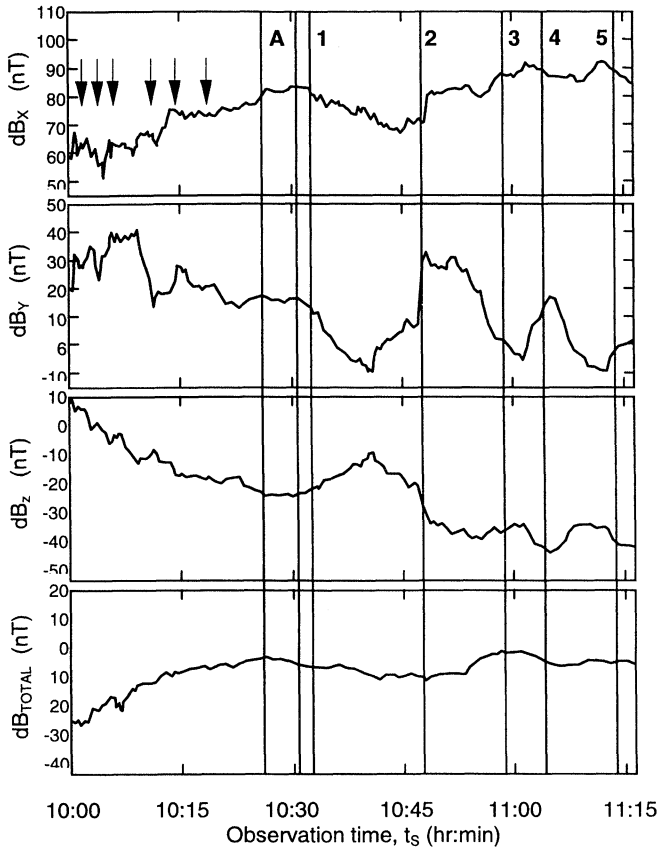

Figure 4. Polar magnetometer observations of the magnetic deflections in the GSM X, Y and Z directions (dB_X, dB_Y, dB_Z) and in the total field dB_{total}. The observed components have been differenced with the predictions of a standard Tsyganenko T96 model (with dynamic pressure of 2 nPa, IMF $B_Y = B_Z = 0$ and a *Dst* index of 0).

about 0900 to 1500 in MLT). Plate 1 of MEA shows that during 0630-1030, the UV aurora at 1500 MLT was moving slowly poleward (because the IMF was northward) but was always at $\Lambda < 80°$. Near 1000 the UV aurora began to move equatorward in response to the southward turning of the IMF. By the time the satellite reached and passed through the cusp region (around 1140 UT, see Plate 1), UVI had ceased making observations. Thus the satellite was always poleward of where the main UV aurora was seen, when it was seen.

Plate 3 shows the UV intensity observed in the afternoon sector by the UVI imager on Polar for 1026-1042 UT. The selected images are for the LBHs filter and are 3 min apart and are integrations over 37-s intervals. The meridian of magnetic noon is the right-hand edge of each plot with radial dotted lines 1 hour of MLT apart. Concentric dotted circles are at magnetic latitudes of 60°, 70° and 80°. On each plot the satellite path for 0900-1200 UT has been plotted, mapped to the ionosphere using a Tsyganenko T89 model for *Kp* of 3. The tick marks give the estimated locations of the satellite footprint at the time of each image. To guide the eye, the same statistical location of the auroral oval has been plotted on each panel as solid lines.

At 1026 UT the clearest of the events discussed by MEA (the event that they labeled as C) is seen breaking away from the poleward edge of the auroral oval. The point where the poleward moving form meets the oval is propagating away from noon, the significance of which is discussed by MEA. The westward end of this feature moves poleward faster than the eastward end, so the arc becomes progressively more aligned with the Y axis. After 1035 it fades, such that it is only just visible at 1042. This arc intersects the mapped satellite footprint at about 1039 UT.

Bright spots in the afternoon sector aurora have been studied by a number of authors (see review by *Liou et al.* [1999] and, despite their very large local time extent, it is possible that events like those shown in Plate 3 may have been classified as bright spots. *Liou et al.* [1999] show that UV bright spots form in a variety of dayside precipitation regions: although they are most likely to be embedded in precipitation classed as plasma sheet, they are also found in the LLBL and polar cap regions.

4. Comparison With the CUTLASS Radar Data

MEA have presented the data from the CUTLASS Finland radar for this period, and compared them with the UVI images. Plate 4 reproduces the latitude-time plots of the radar echoes seen in beams 3, 7 and 13 (near the western edge, center and eastern edge, respectively, of the field of view of the CUTLASS Finland radar). The color coding shows the Doppler velocities (red being away from the radar at 1 km s^{-1}). We have added the magnetic latitude of the mapped ionospheric footprint of the satellite, with the locations of the steps marked. In addition, the time that Polar exited from the initial cusp at 1010 is marked, along with 1135-1145 when Polar passed through the cusp for the last time.

The cusp crossing agrees well with the latitudes that backscatter is seen in beam 3. However, the satellite pass is at MLT near 1500 and lies between beams 7 and 13. In these two beams the mapped footprint of the cusp intersection is at slightly higher latitude than the radar echoes. From this, we infer that the true satellite footprint is approximately 2° equatorward of the location predicted by the field line model. Such an error is entirely consistent with the uncertainty in the field line mapping over a distance of about 4 R_E.

With or without this inferred shift in latitude, steps 1, 2 and 3 fall on the extrapolated path of the major poleward moving events seen in beams 3 and 17. However, the 2° shift is required if these steps are to also coincide with the events in beam 13 (but note that only the first event is completely clear in this radar beam). Neither the upward ramp 4 nor the small step 5 show a clear signature in the CUTLASS data. Note that there is no signature of the cusp seen by Polar before 1010. This is presumably because it was at higher latitudes and no HF propagation paths were possible that gave near perpendicularity to the field-aligned irregularities in the cusp region. If so, this demonstrates how the operation frequency of HF radar can introduce selection effects into the data accrued.

With the 2° shift of the predicted satellite footprint inferred above, the field line of poleward moving arc in Figure 4 intersects the satellite field line just before 1035. Rather than the arc moving right over the satellite footprint, the arc fades at the satellite location after about 1039 UT.

5. Discussion

The sawtooth signatures of the ion data reveal pulses in the rate of the reconnection that gives magnetosheath ions entry into the magnetosphere. The largest step at 1035-1040 UT

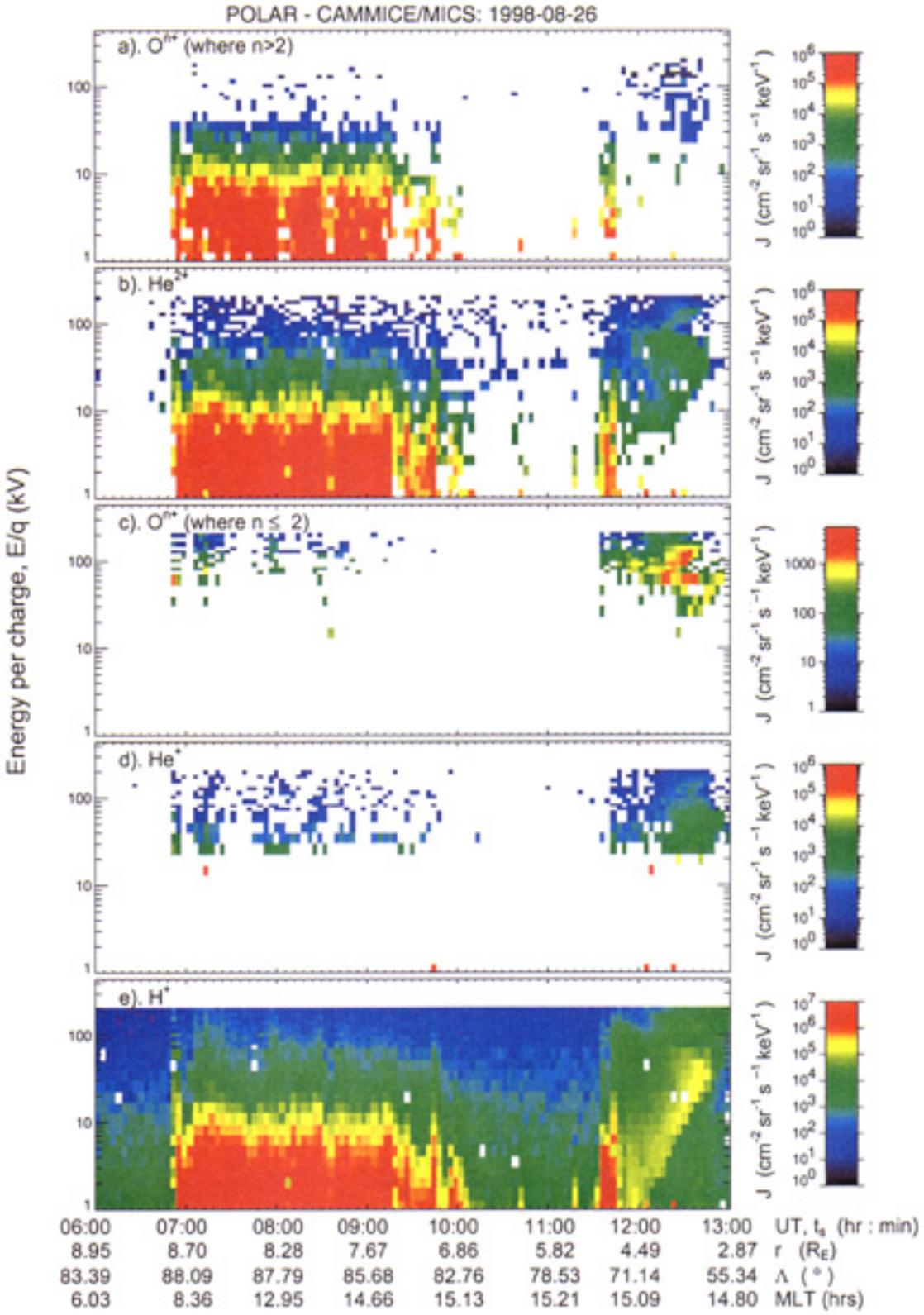

Plate 1. Observations by the Charge and Mass Magnetospheric Ion Composition Experiment (CAMMICE) on the Polar satellite of the differential number flux of ions in an energy per charge-observation time spectrogram format. (a) O^{n+} ions where the charge state n exceeds 2 (predominantly of solar origin). (b) He^{2+} ions (predominantly of solar origin). (c) O^{n+} ions where the charge state n is 2 or less (predominantly of ionospheric origin). (d) He^{+} ions (predominantly of magnetospheric origin). (e) H^{+} ions. The satellite location at every universal time (UT) of observation, t_s, is given in terms of geocentric distance r, invariant latitude Λ, and magnetic local time, MLT.

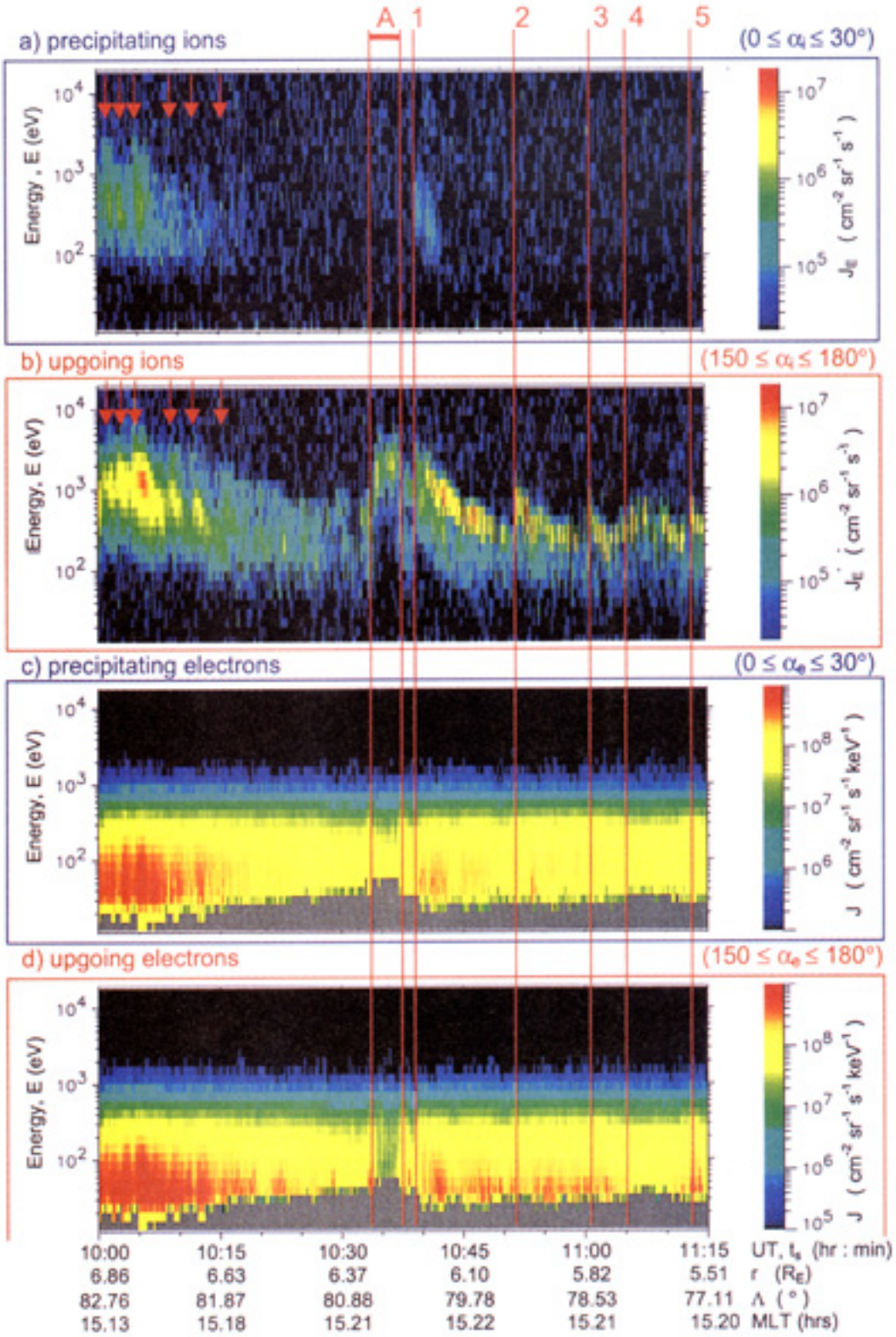

Plate 2. Observations by the Hydra instrument on Polar of particle populations shown in energy-observation time spectrogram format. (a) Differential energy fluxes of precipitating ions (with pitch angles α_i between 0° and 30°). (b) Differential energy fluxes of upgoing ions (150° < α_i < 180°). (c) Differential number fluxes of precipitating electrons (0° < α_e < 30°). (d) Differential number fluxes of upgoing electrons (150° < α_e < 180°). The vertical red lines mark the putative arc feature (labeled A) and cusp ion steps 1-5. The arrows denote smaller cusp ion steps due to shorter period reconnection pulses. The satellite location at every universal time (UT) of observation, t_s, is given in terms of geocentric distance r, invariant latitude Λ, and magnetic local time MLT.

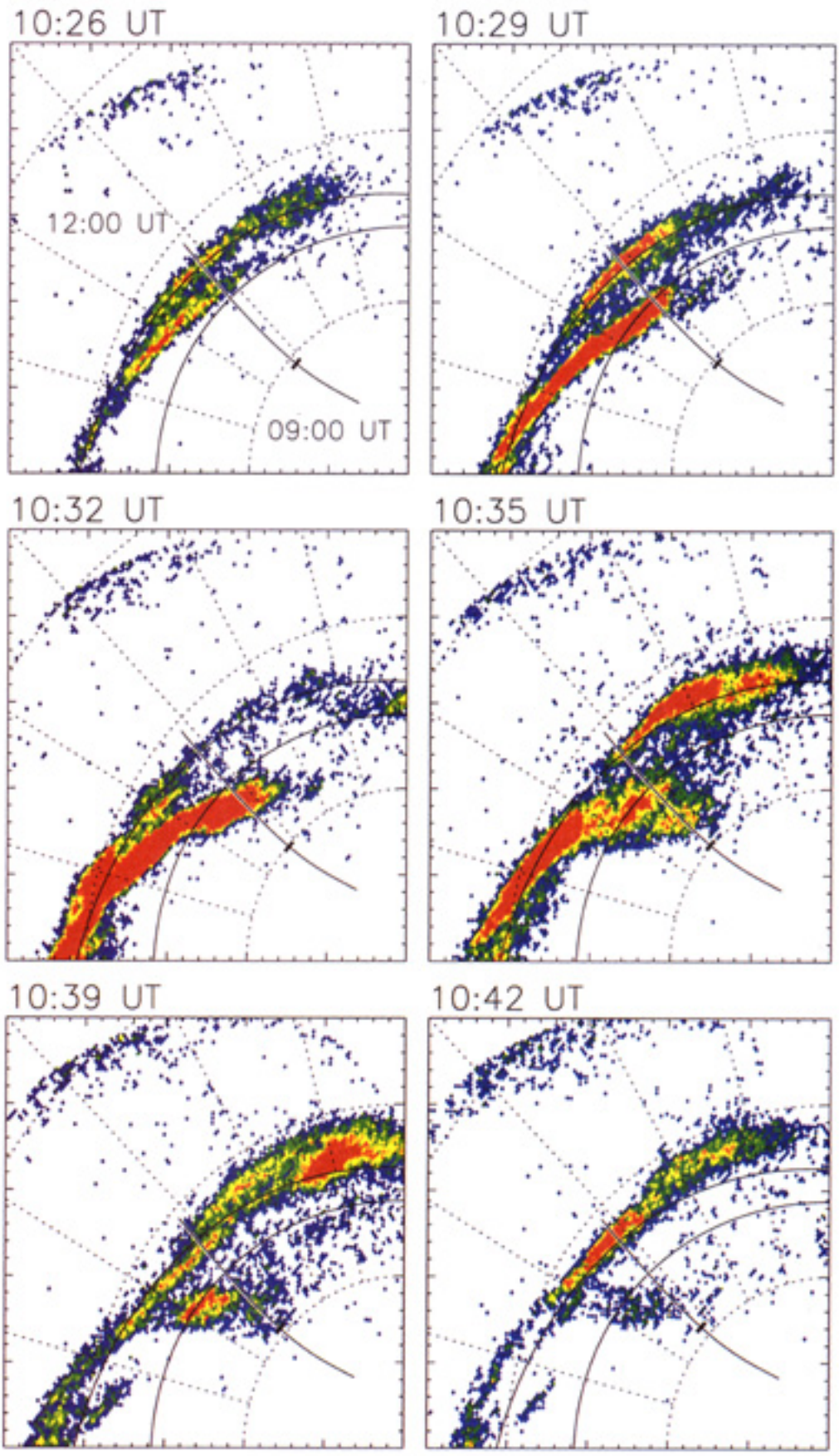

Plate 3. Polar UVI images for 1026-1042 UT. The line shows the Polar trajectory for 0900-1200, mapped to the ionosphere using a Tsyganenko T93 field line model with Kp = 3. The marks show the predicted footprint location at the time of each image.

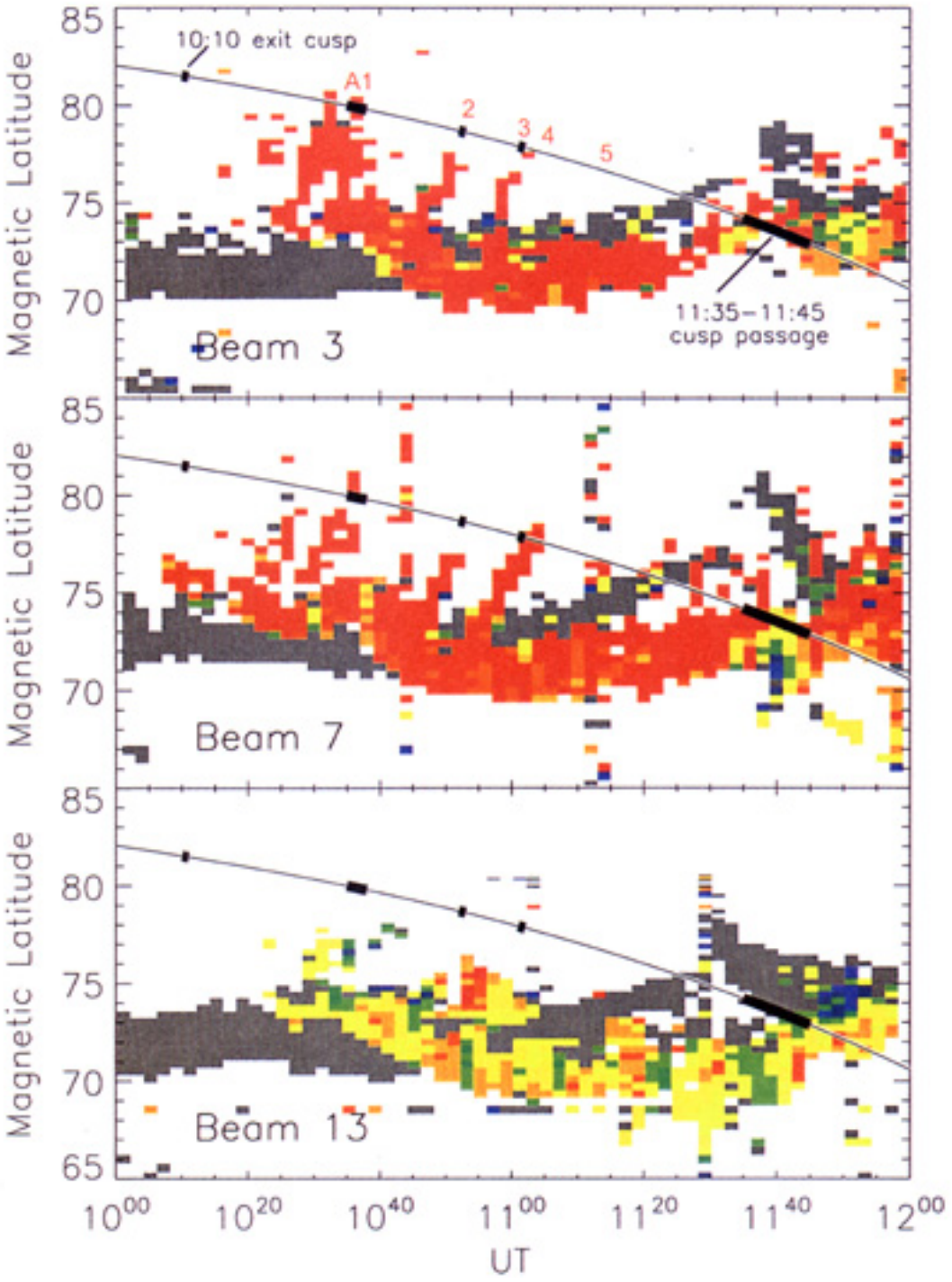

Plate 4. Doppler shifts seen by the Cooperative UK Twin Located Auroral Sounding System (CUTLASS) Finland radar in beam 3 (to the west of the field of view), beam 7 (near the center of the field of view), and beam 13 (to the east of the field of view), shown as a function of magnetic latitude and time. Grey areas are zero Doppler shift echoes caused by ground scatter. On each panel the magnetic latitude of the Polar satellite has been marked and the times of various observed features given. Prior to 1010 UT, Polar was in a high-latitude cusp, but no signature of this is seen in the HF radar data. At 1135-1145 Polar passed through the cusp again, this time at a lower latitudes. This southward IMF cusp agrees with the band of HF backscatter echoes, to within the uncertainty in the field line mapping. The arc feature A and the major steps 1, 2 and 3 are also marked and are seen to line up with poleward moving events seen by the HF radar.

has a double form in the upgoing ions (Plate 2b). This could be caused by a solar wind pressure pulse compressing the geomagnetic field and moving a single cusp ion step such that it passes over the satellite three times [*Lockwood et al.*, 1998]. However, this would necessarily cause the same double structure to be seen in downgoing ions, and inspection of Plate 2a clearly shows that this is not the case. We also note that the first feature, but not the second, is accompanied by a dropout in upgoing electrons (Plate 2d). We conclude that this structure is not the same step intersected twice, nor is it two steps.

The observed magnetic perturbation ΔB_Y in Figure 4 shows upward field-aligned current throughout 1034-1040, but this current is structured, with smaller values of ΔB_Y at the time of the first ion feature. We here propose that this feature is, in fact, a single cusp ion step feature (labeled 1 in Plate 2), surrounded by its associated upward current sheet (as predicted for the mantle region with IMF $B_Y > 0$). This current is found on the last of the field lines to be opened in the first reconnection pulse (seen just before the step) and on the first of the field lines to be reconnected in the second pulse (seen just after the step). Because of the time-of-flight effects, the plasma concentration on the former field lines will be much smaller than on the latter field lines. If the upward $J_\parallel$ is carried predominantly by the downgoing magnetospheric electrons, these would need to move faster on the field lines seen just before the step, and we propose that in this region the electron flow has become unstable and produced a parallel potential drop of about 1 kV beneath the satellite in the region labeled A in Plate 2. This has accelerated the upgoing ions by about 1 keV and broadened the electron loss cone to about 11° (from the 4° predicted by the Tsyganenko magnetic field model for adiabatic electron motion). This gives the dropout in the fluxes of upgoing electrons, without changing the downgoing electrons. This would also produce 1-keV precipitating electrons at the top of the atmosphere that would have produced the UV auroral arc that the satellite footprint intersects near this time.

The second feature in the upgoing ions (near 1040 UT, labeled 1 in Plate 2 and Figure 4) is thus the actual cusp ion step, and this is marked by the reappearance of precipitating ions and a strong upward field-aligned current sheet. The lower cutoff in these upgoing ions is difficult to define because of smearing caused by the dependence of the mirror height on pitch angle. The best estimate that we can make is from the ions on the edge of the loss cone, giving a step in the lower cutoff from 50 to 200 eV. If we take a nominal distance from the magnetopause to the mirror point of 15 R_E and a further 6 R_E from the mirror point back up to the satellite, this gives a change in elapsed time since reconnection of $(t_o - t_s)$ from 22 to 11 min. In other words, the step is produced by a period of about 11 min of near-zero reconnection rate (1013-1024 UT).

We note that all other steps, despite showing accompanying signatures in the magnetometer data consistent with the motion of field-aligned current sheets over the satellite, have no definable signature in the electron data. In these cases, the current appears to be carried by electrons out of the range of the detector (<10 eV and/or >20 MeV). As there is no significant structure above about 1 MeV, it is most likely that electrons below 10 eV are the dominant electron carriers in all cases, other than step 1.

As interpreted by MEA, the UV arc seen at 1026 and 1029 in Plate 3 initially marks the antisunward edge of the patch of newly opened flux. It is the region of upward field-aligned current associated with the westward motion of the event. As the curvature force on the newly opened field lines decays, the motion evolves to antisunward, and this field-aligned current migrates to the eastward end of the event, as illustrated by *Lockwood et al.* [1993a] and MEA. This is consistent with the motion of the brightest luminosity in this arc shown in Plate 3. We also note that Figure 1b predicts that the strongest upward field-aligned current associated with each event will be at the eastward end of the event where it is not contiguous with the prior event. Thus the westward end of the arc may mark the eastern end of the patch of newly opened flux generated by the previous reconnection pulse.

Plate 2 of MEA shows that the UV arcs seen in this MLT sector form a series of poleward moving events. Thus both major arcs seen at 1200-1600 MLT in Plate 3 are consistent with events at different stages of their evolution: This being the case, both these UV arcs are caused by the difference of longitudinal speeds of adjacent patches associated with the tension force on newly opened field lines. The lower-latitude arc is the boundary between the more recently-produced patches of newly opened flux . Plate 3 shows that the UV arcs have considerable variation as the patches of newly opened flux evolve.

The field-aligned current $J_\parallel$ will be larger if the difference between the velocities of the two patches is larger, which will increase with the difference in time elapsed since reconnection $(t_o - t_s)$ and thus with the size of the step in ion energy. The longer the interval of near-zero reconnection, the larger the $J_\parallel$ that is required at the step. This explains why a strong arc feature formed across the largest step in Plate 2, but only weak features are seen in association with the smaller steps. Stronger field-aligned currents will also be present if the IMF B_Y component is larger, and thus such UV arcs should be more readily observed in such cases. As events evolve into the polar cap the difference in the longitudinal motion speed decays and so the $J_\parallel$ at the step will also decay and any arc associated with a step will fade.

We also note that for negative IMF B_Y, the field-aligned current required on the steps will be downward. Such downward currents may be readily supplied by upgoing ionospheric electrons, and the parallel potential drop and the UV arc may not form in such cases. This would restrict UV observations of poleward moving arcs to cases with a strong positive IMF B_Y component only.

6. Conclusions

Cusp ion steps in the mantle region have been shown to be coincident with field-aligned current sheets, consistent with our predictions of pulsed magnetopause reconnection an IMF that has a large B_Y component. If the delay between successive reconnection pulses is large, the field-aligned current, for large positive IMF B_Y component at least, can go unstable and produce a poleward moving arc feature on open field lines that can be imaged by global UV images.

The results confirm that the events seen in HF radar data and UV images by MEA are indeed due to pulsed reconnection. That being the case, the large longitudinal extents of the events mean that each contributes 10% of the total polar cap

flux and that these events are indeed responsible for all of the transpolar voltage (and thus the polar cap expansion) at this time. In addition, the evolution of the events is therefore consistent with the moving or expanding active X-line segment, as proposed by *Lockwood et al.* [1993b] and *Lockwood* [1994].

Acknowledgements. The work of M.L., C.H.P. and S.E.M. is funded by the U.K. Particle Physics and Astronomy Research Council (PPARC). CUTLASS is supported by PPARC (grant PPA/R/R/1997/00256), the Swedish Institute for Space Physics (IRF), Uppsala, and the Finnish Meteorological Institute, Helsinki.

Michel Blanc thanks Jean-Michel Bosqued and Jøran Moen for their assistance in evaluating this paper.

References

Burch, J. L., Quasi-neutrality in the polar cusp, *Geophys. Res. Lett., 12,* 469-472, 1985.

Cowley, S.W.H., and M. Lockwood, Excitation and decay of solar-wind driven flows in the magnetosphere-ionosphere system, *Ann. Geophys., 10,* 103-115, 1992.

Cowley, S.W.H., M.P. Freeman, M. Lockwood and M.F. Smith, The ionospheric signature of flux transfer events, *CLUSTER - Dayside Polar Cusp",* edited by C.I. Barron, *Euro. Space Agency Publ., ESA SP-330,* 105-112, 1991b.

Davis, C.J., and M. Lockwood, Predicted signatures of pulsed reconnection in ESR data, *Ann. Geophys., 14,* 1246-1256, 1996

Elphic, R.C., M. Lockwood, S.W.H. Cowley, and P.E. Sandholt, Flux transfer events at the magnetopause and in the ionosphere, *Geophys. Res. Lett., 17,* 2241-2244, 1990.

Escoubet, C.P., M.F. Smith, S.F. Fung, P.C. Anderson, R.A. Hoffman, E.M. Basinska, and J.M. Bosqued, Staircase ion signature in the polar cusp: A case study, *Geophys. Res. Lett., 19,* 1735-1738, 1992.

Farrugia, C.J., P.E. Sandholt, W.F. Denig, and R.B. Torbert, Observation of a correspondence between poleward moving auroral forms and stepped cusp ion precipitation, *J. Geophys. Res., 103,* 9309-9315, 1998.

Fasel, G.J., Dayside poleward moving auroral forms: A statistical study, *J. Geophys. Res., 100,* 11,891-11,905, 1995.

Haerendel, G., G. Paschmann, N. Sckopke, H. Rosenbauer, and P. C. Hedgecock, The frontside boundary layer of the magnetopause and the problem of reconnection, *J. Geophys. Res., 83,* 3195-3216, 1978.

Karlson, K.A., M. Øieroset, J. Moen, and P.E. Sandholt, A statistical study of flux transfer event signatures in the dayside aurora: The IMF B_Y-related postnoon-prenoon asymmetry, *J. Geophys. Res., 101,* 59-68, 1996.

Kawano, H., and C.T. Russell, Survey of flux transfer events observed with the ISEE spacecraft: Rotational polarity and the source region, *J. Geophys. Res., 101,* 27,299-27,308, 1996.

Kawano, H., and C.T. Russell, Survey of flux transfer events observed with the ISEE spacecraft: Dependence on the interplanetary magnetic field, *J. Geophys. Res., 102,* 11,307-11,313, 1997

Liou, K., P. T. Newell, C.-I. Meng, T. Sotirelis, M. Brittnacher, and G. Parks, Source region of 1500 MLT auroral bright spots: Simultaneous polar UV-images and DMSP particle data, *J. Geophys. Res., 104,* 24,587-24,602, 1999.

Lockwood, M., Ionospheric signatures of pulsed magnetopause reconnection, *in "Physical signatures of magnetopause boundary layer Processes",* edited by J.A. Holtet and A. Egeland, *NATO ASI Ser., Ser. C, 425,* 229-243, 1994.

Lockwood, M., The location and characteristics of the reconnection X-line deduced from low-altitude satellite and ground-based observations: 1. Theory, *J. Geophys. Res., 100,* 21,791-21,802, 1995.

Lockwood, M., Energy and pitch angle dispersions of LLBL/cusp ions seen at middle altitudes: Predictions by the open magnetosphere model, *Ann. Geophys., 15,* 1501-1511, 1997.

Lockwood, M., and C.J. Davis, On the longitudinal extent of magnetopause reconnection bursts, *Ann. Geophys., 14,* 865-878, 1996.

Lockwood, M., and M.A. Hapgood, On the cause of a magnetospheric flux transfer event, *Geophys. Res., 103,* 26,453-26,478, 1998.

Lockwood, M., and M.F. Smith, The variation of reconnection rate at the dayside magnetopause and cusp ion precipitation, *J. Geophys. Res., 97,* 14,841-14,847, 1992.

Lockwood, M., M.O. Chandler, J.L. Horwitz, J.H. Waite Jr., T.E. Moore, and C.R. Chappell, The cleft ion fountain, *J. Geophys. Res., 90,* 9736-9748, 1985a.

Lockwood, M., T.E. Moore, J.H. Waite, C.R. Chappell, J.L. Horwitz, and R.A. Heelis, The geomagnetic mass spectrometer - Mass and energy dispersions of ionospheric ion flows into the magnetosphere, *Nature, 316,* 612-613, 1985b.

Lockwood, M., P.E. Sandholt, and S.W.H. Cowley, Dayside auroral activity and momentum transfer from the solar wind, *Geophys. Res. Lett., 16,* 33-36, 1989a.

Lockwood, M., P.E. Sandholt, S.W.H. Cowley, and T. Oguti, Interplanetary magnetic field control of dayside auroral activity and the transfer of momentum across the dayside magnetopause, *Planet. Space Sci., 37,* 1347-1365, 1989b.

Lockwood, M., S.W.H. Cowley, P.E. Sandholt, and R. P. Lepping, The ionospheric signatures of flux transfer events and solar wind dynamic pressure changes, *J. geophys. Res., 95,* 17,113-17,136, 1990.

Lockwood, M., H.C. Carlson, and P.E. Sandholt, The implications of the altitude of transient 630 nm dayside auroral emissions, *J. Geophys. Res., 98,* 15,571-15,587, 1993a.

Lockwood, M., J. Moen, S.W.H. Cowley, A.D. Farmer, U.P. Løvhaug, H. Lühr, and V.N. Davda, Variability of dayside convection and motions of the cusp/cleft aurora, *Geophys. Res. Lett., 20,* 1011-1014, 1993b.

Lockwood, M., W.F. Denig, A.D. Farmer, V.N. Davda, S.W.H. Cowley and H. Lühr, Ionospheric signatures of pulsed magnetic reconnection at the Earth's magnetopause., *Nature, 361,* 424-428, 1993c.

Lockwood, M., S.W.H. Cowley, P.E. Sandholt, and U.P. Løvhaug, Causes of plasma flow bursts and dayside auroral transients: An evaluation of two models invoking reconnection pulses and changes in the Y-component of the magnetosheath field, *J. Geophys. Res., 100,* 7613-7626, 1995a.

Lockwood, M., S.W.H. Cowley, M.F. Smith, R.P. Rijnbeek and R.C. Elphic, The contribution of flux transfer events to convection, *Geophys. Res. Lett., 22,* 1185-1188, 1995b.

Lockwood, M., C.J. Davis, T.G. Onsager, and J.A. Scudder, Modeling signatures of pulsed magnetopause reconnection in cusp ion dispersion signatures seen at middle altitudes, *Geophys. Res. Lett., 25,* 591-594, 1998.

Lockwood, M., I.W. McCrea, S.E. Milan, J. Moen, J.C. Cerisier and A. Thorolfsson, Plasma structure within poleward-moving cusp-cleft auroral transients: EISCAT Svalbard radar observations and an explanation in terms of large local time extent of events, *Ann. Geophys., 18,* 1027-1042, 2000.

Milan S. E., M. Lester, S. W. H. Cowley, J. Moen, P. E. Sandholt, and C. J. Owen, Meridian-scanning photometer, coherent HF radar, and magnetometer observations of the cusp: a case study, *Ann. Geophysicae, 17,* 159-172, 1999.

Milan, S.E., M. Lester, S.W.H. Cowley, and M. Brittnacher, Convection and auroral response to a southward turning of the IMF: Polar UVI, CUTLASS and IMAGE signatures of transient magnetic flux transfer at the magnetopause, *J. Geophys. Res., 105,* 15,741-15,755, 2000.

Moen, J., P.E. Sandholt, M. Lockwood, W.F. Denig, U.P. Løvhaug, B. Lybekk, A. Egeland, D. Opsvik, and E. Friis-Christensen, Events of enhanced convection and related dayside auroral activity, *J. Geophys. Res., 100,* 23,917-23,934, 1995.

Moen, J., M. Lockwood, P.E. Sandholt, U.P. Løvhaug, W.F. Denig, A.P. van Eyken, and A. Egeland, Variability of dayside high-latitude convection associated with a sequence of auroral transients, *J. Atmos. Terr. Phys., 58,* 85-96, 1996.

Neudegg, D.A., T.K. Yeoman, S.W.H. Cowley, G. Provan, G. Haerendel, W. Baumjohann, U. Auster, K.-H. Fornacon, E. Georgescu, and C.J. Owen, A flux transfer event observed at the magnetopause by the equator-S spacecraft and in the ionosphere by the CUTLASS HF radar, *Ann. Geophys., 17,* 707-711, 1999.

Newell, P.T., and D.G. Sibeck, Upper limits on the contribution of flux transfer events to ionospheric convection, *Geophys. Res. Lett. 20,* 2829-2832, 1993.

Øieroset, M., H. Lühr, J. Moen, T. Moretto, and P.E. Sandholt, Dynamical auroral morphology in relation to ionospheric convection

and geomagnetic activity: Signatures of magnetopause X-line dynamics and flux transfer events, *J. Geophys. Res., 101*, 13,275-13,292, 1996.

Øieroset, M., P.E. Sandholt, H. Lühr, W.F. Denig, and T. Moretto, Auroral and geomagnetic events at cusp/mantle latitudes in the prenoon sector during positive IMF B_Y conditions: Signatures of pulsed magnetopause reconnection, *J Geophys. Res., 102*, 7191-7205, 1997.

Onsager, T.G., C.A. Kletzing, J.B. Austin, and H. MacKiernan, Model of magnetosheath plasma in the magnetopshere: Cusp and mantle particles at low altitudes, *Geophys. Res. Lett., 20,* 479-482, 1993.

Pinnock, M., A.S. Rodger, J.R. Dudeney, K.B. Baker, P.T. Newell, R.A. Greenwald, and M.E. Greenspan, Observations of an enhanced convection channel in the cusp ionosphere, *J. Geophys. Res., 98,* 3767-3776, 1993.

Pinnock, M., A.S. Rodger, J.R. Dudeney, F. Rich, and K.B. Baker, High spatial and temporal resolution observations of the ionospheric cusp, *Ann. Geophys., 13*, 919-925, 1995.

Provan, G., and T.K. Yeoman, Statistical observations of the MLT, latitude and size of pulsed ionopheric flows with CUTLASS Finland radar, *Ann. Geophys., 17*, 855-867, 1999.

Provan, G., T.K. Yeoman, and S.E. Milan, CUTLASS Finland radar observations of the ionospheric signatures of flux transfer events and resulting plasma flows, *Ann. Geophys., 16*, 1411-1422, 1998.

Provan, G., T. K. Yeoman, and S. W. H. Cowley, The influence of the IMF B_Y component on the location of pulsed ionospheric flows in the dayside ionosphere observed by HF radars, *Geophys. Res. Lett., 26*, 521-5124, 1999.

Rodger, A.S., S.B. Mende, T.J. Rosenberg, and K.B. Baker, Simultaneous optical and HF radar observations of the ionospheric cusp, *Geophys. Res. Lett., 22*, 2045-2048, 1995.

Rosenbauer, H., H. Grünwaldt, M.D. Montgomery, G. Paschmann, and N. Skopke, HEOS-2 plasma observations in the distant polar magnetosphere: The plasma mantle, *J. Geophys. Res., 80,* 2723-2737, 1975.

Russell, C. T., and R. C. Elphic, Initial ISEE magnetometer results: Magnetopause observations, *Space Sci. Rev., 22,* 681-715, 1978.

Russell, C. T., and R. C. Elphic, ISEE observations of flux transfer events at the dayside magnetopause, *Geophys. Res. Lett., 6,* 33-36, 1979.

Sandholt, P.E., M. Lockwood, W.F. Denig, R.C. Elphic, and S. Leontjev, Dynamical auroral structure in the vicinity of the polar cusp: Multipoint observations during southward and northward IMF, *Ann. Geophys., 10,* 483-497, 1992.

Saunders, M.A., The origin of cusp Birkeland currents, *Geophys. Res. Lett., 16,* 151-154, 1989.

Scholer, M., Magnetic flux transfer at the magnetopause based on single X-line bursty reconnection, *Geophys. Res. Lett., 15,* 291-294, 1988.

Scholer, M., Asymmetric time-dependent and stationary magnetic reconnection at the dayside magnetopause, *J. Geophys. Res., 94,* 15,099-15,111, 1989.

Siscoe, G.L., and T.S. Huang, Polar cap inflation and deflation, *J. Geophys. Res., 90*, 543-547, 1985.

Southwood, D. J., Theoretical aspects of ionosphere-magnetosphere-solar wind coupling, *Adv. Space Res., 5(4),* 7-14, 1985.

Southwood, D. J., The ionospheric signature of flux transfer events, *J. Geophys. Res., 92,* 3207-3213, 1987.

Southwood, D. J., C. J. Farrugia, and M. A. Saunders, What are flux transfer events?, *Planet. Space Sci., 36,* 503-508, 1988.

Walker, I. K., J. Moen, C. N. Mitchell, L. Kersley, and P.E. Sandholt, Ionospheric effects of magnetopause reconnection observed using ionospheric tomography, *Geophys. Res. Lett., 25,* 293-296, 1998.

Yeoman, T.K., M. Lester, S.W.H. Cowley, S.E. Milan, J. Moen, and P.E. Sandholt, Simultaneous observations of the cusp in optical, DMSP and HF radar data, *Geophys. Res. Lett., 24*, 2251-2254, 1997.

M. Brittnacher, Geophysics Program, University of Washington, Box 351650, Seattle, WA 98195. (britt@geophys.washington.edu)

M. Lockwood nd C.H. Perry, Space Science and Technology Department, Rutherford Appleton Laboratory, Chilton, Didcot, Oxfordshire, OX11 0QX, England, UK. (m.lockwood@rl.ac.uk, c.h.perry@rl.ac.uk)

S.E. Milan, Radio and Space Plasma Physics Group, Department of Physics and Astronomy, Leicester University, University Road, Leicester, Leicestershire, LE1 7RH, England, UK. (ets@ion.le.ac.uk)

T. Onsager, NOAA Space Environment Center, 325 Broadway, Boulder, CO 80303. (terry.onsager@noaa.gov)

C.T. Russell, Institute of Geophysics and Planetary Physics, Space Science Center, University of California Loa Angeles, 405 Hilgard Avenue, Los Angeles, CA 900254-1567. (ctrussell@igpp.ucla.edu)

J. D. Scudder, Dept Physics & Astronomy, University of Iowa, Van Allen Hall, Iowa City, IA 52240. (jds@hydra.physics.uiowa.edu)

(Received January 3, 2000; revised November 22, 2000; accepted December 7, 2000.)